*36th EPS Conference on Plasma Phys. Sofia, June 29 - July 3, 2009 ECA Vol.**33E**, P-4.120 (2009)*

The effects of non-uniform magnetic field strength on test particle transport in drift wave turbulence

J M Dewhurst[1], B Hnat[1] and R O Dendy[2,1]

[1]*Centre for Fusion, Space and Astrophysics, University of Warwick, Coventry CV4 7AL, U.K.*

[2]*Euratom/UKAEA Fusion Association, Culham Science Centre, Oxfordshire OX14 3DB, U.K.*

Introduction. It is generally agreed that drift wave turbulence is a good candidate to explain the observed transport in fusion devices from first principles. In tokamaks, toroidal curvature leads to a non-uniform magnetic field strength which alters the properties of the turbulence, allowing the excitation of interchange-type ballooning modes. Here, we investigate the effects of a non-uniform magnetic field on the turbulence and the transport of passive test particles using direct numerical simulation.

Model equations. Our model of drift wave turbulence is an extended form of the Hasegawa-Wakatani (HW) model that includes a magnetic field inhomogeneity in the radial direction and the resulting resistive interchange driven modes. The equations for density n and vorticity $\nabla^2\phi$, where ϕ is the electrostatic potential, are

$$\frac{\partial n}{\partial t} = -\kappa\frac{\partial \phi}{\partial y} + \alpha(\phi - n) + [n,\phi] + C\frac{\partial}{\partial y}(\phi - n) + \mu\nabla^2 n\,, \tag{1}$$

$$\frac{\partial}{\partial t}(\nabla^2\phi) = \alpha(\phi - n) + \left[\nabla^2\phi,\phi\right] - C\frac{\partial n}{\partial y} + \mu\nabla^2(\nabla^2\phi)\,, \tag{2}$$

where the magnetic field inhomogeneity is controlled by the parameter $C = -\partial \ln B/\partial x$. The standard HW equations are recovered when $C = 0$. The equations can be rewritten in the form of a diffusion equation, $d\Pi/dt = \mu\nabla^2\Pi$, where Π is the potential vorticity,

$$\Pi = \nabla^2\phi - n + (\kappa - C)x\,. \tag{3}$$

In the inviscid limit, $\mu = 0$, the potential vorticity is a Lagrangian conserved quantity.

We solve Eqs. (1) and (2) on a square of length $L = 40$ using 256×256 grid nodes with periodic boundary conditions. We are interested in the effects of changing the the parameter C and therefore set $\alpha = 0.5$, $\kappa = 1$, $\mu = 0.01$ throughout.

Probe measurements. We record the $E \times B$ radial density flux, $\Gamma_n = nv_x = -n\partial\phi/\partial y$, density n, potential ϕ and radial velocity $v_x = -\partial\phi/\partial y$ at one grid-node (i.e. point-wise) during the quasi-stationary turbulent state. From the Γ_n time series we compute its probability density function (PDF) $P(\Gamma_n)$, and quantify departures of the distribution from Gaussian with skewness $S = \langle\Gamma_n^3\rangle/\langle\Gamma_n^2\rangle^{3/2}$, measuring asymmetry, and kurtosis $K = \langle\Gamma_n^4\rangle/\langle\Gamma_n^2\rangle^2$, measuring peakedness; a Gaussian PDF has $S = 0$ and $K = 3$. Fig. 1(a) shows the PDFs $P(\Gamma_n)$ for three different values of C. All three are clearly non-Gaussian and are skewed towards positive radial flux.

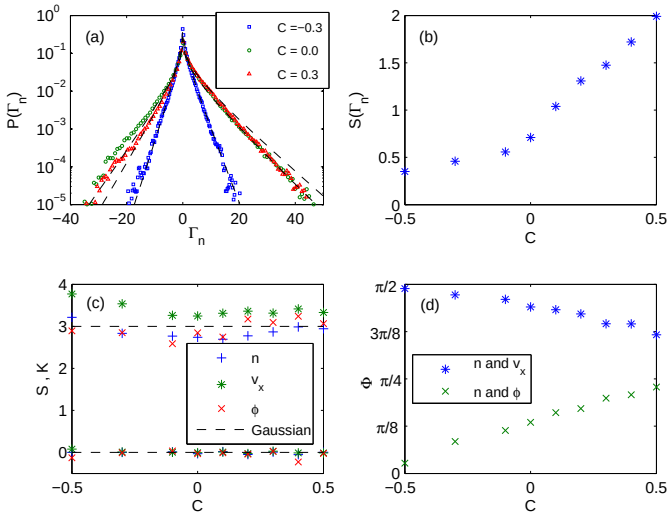

Figure 1: (a) PDFs and (b) skewness of PDFs of the point-wise radial density flux $\Gamma_n = nv_x$ for different values of C. The dashed lines over the PDFs are the PDFs calculated using Eqs. (4) and (5) and probe data from the simulation. (c) Skewness and kurtosis of PDFs of point-wise density n, radial velocity v_x and potential ϕ. (d) Relative phase between n and v_x, and between n and ϕ.

In Fig. 1(b), we plot the skewness of the PDFs for a wider range of C, increasing C monotonically increases the skewness of Γ_n. In Fig. 1(c) we plot S and K for the point-wise measurements of n, ϕ and v_x. These quantities are very close to Gaussian for the full range of C. For the case where the amplitudes of the fluctuations in radial velocity v_x and density n are exactly Gaussian, the PDF of radial turbulent flux $\Gamma_n = nv_x$ can be shown to be [1]

$$P(\Gamma_n) = \frac{1}{\pi}\frac{\sqrt{1-\gamma^2}}{\sigma_v\sigma_n} K_0\left(\frac{|\Gamma_n|}{\sigma_v\sigma_n}\right)\exp\left(-\gamma\frac{\Gamma_n}{\sigma_v\sigma_n}\right), \tag{4}$$

where σ_v and σ_n are the standard deviations of velocity and density fluctuations, K_0 is the modified Bessel function of the second kind and γ is a parameter that measures the correlation between v_x and n,

$$\gamma = -\frac{\langle v_x n\rangle}{\langle v_x^2\rangle^{1/2}\langle n^2\rangle^{1/2}} \equiv -\cos\Phi\,, \tag{5}$$

where Φ is the average relative phase between v_x and n. In Fig. 1(d) we plot the relative phase Φ between v_x and n, and also between ϕ and n, showing that Φ changes roughly linearly with C. We conclude that changing C alters the relative phase between fluctuations in n and ϕ, which leads to the observed change in the skewness of the flux PDF. In Fig. 1(a) we overlay with dashed lines the PDFs calculated using Eqs. (4) and (5) and probe data from the simulation. Moderately good agreement is found, indicating that the quantities v_x and n are indeed close to Gaussian.

Test particle transport. Ten thousand test particles are initialised at random once a quasi-stationary turbulent state has been reached. The test particle equation of motion is $\partial\mathbf{r}/\partial t = \mathbf{v}_E(\mathbf{r})$, where $\mathbf{v}_E = (-\partial\phi/\partial y, \partial\phi/\partial x)$ is the $E\times B$ velocity. We calculate running diffusion coefficients in the radial x and poloidal y directions separately, $D_x(t) = X(t)^2/2t$ and $D_y(t) = Y(t)^2/2t$. Here $X(t)^2 = \langle[x(t) - \langle x(t)\rangle]^2\rangle$, $Y(t)^2 = \langle[y(t) - \langle y(t)\rangle]^2\rangle$ and $(x(t), y(t))$ is the position of the particle with respect to its initial position; angular brackets denote an ensemble average over the $10,000$ test particles. For an ordinary diffusive process the running diffusion

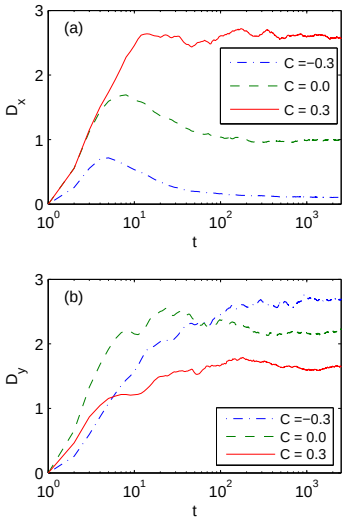

Figure 2: (a) D_x and (b) D_y versus time for different C.

coefficient will reach a value independent of time since $X(t)^2 \sim t$. More generally the transport may be 'anomalous' and $X(t)^2 \sim t^\sigma$, where $0 < \sigma < 1$ implies subdiffusion, $1 < \sigma < 2$ implies superdiffusion and $\sigma = 2$ is ballistic.

In Fig. 2 we plot D_x and D_y as functions of time for $C = [-0.3, 0.0, 0.3]$. In all cases, after a short initial ballistic phase, the running diffusion coefficient asymptotically tends to a value independent of time, indicating a diffusive process. Increasing the parameter C tends to increase the radial diffusion coefficient D_x and decrease the poloidal one D_y. For $C = 0$ and $C = -0.3$ we find that the poloidal diffusion is stronger than the radial; however, for $C = 0.3$ this anisotropy is reversed and the radial diffusion dominates. In Fig. 3 we plot $X^2/t^{0.45}$ and $Y^2/t^{1.7}$ versus time for $C = -0.5$. We find that, after an initial phase, these quantities become time independent, indicating that the radial test particle transport is subdiffusive with exponent $\sigma \approx 0.45$ and the poloidal transport is superdiffusive with $\sigma \approx 1.7$.

Fig. 4(a) displays the time-independent values of D_x and D_y for a wider range of C (for cases where the transport is diffusive). We find that D_x increases and D_y decreases with C. We also plot the total radial density flux Γ_{n0} averaged over the computational box in Fig. 4(b). Extending the arguments in Ref. [2], Γ_{n0} and D_x can be linked through conservation of potential vorticity Π. We infer [3]

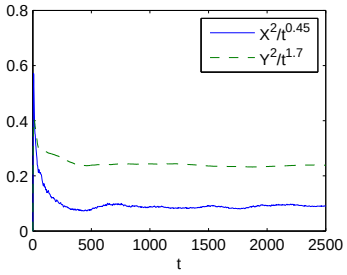

Figure 3: Plots of $X^2/t^{0.45}$ and $Y^2/t^{1.7}$ versus time for $C = -0.5$.

$$\Gamma_{n0} = (\kappa - C) D_x \,, \tag{6}$$

which is in the form of Fick's law. In Fig. 4(b) we plot $(\kappa - C)D_x$ which closely matches Γ_{n0}. Thus we may use Eq. (6) to link the radial diffusive transport of test particles to the underlying turbulence. Interestingly, the expression includes the factor $\kappa - C$, which can be shown to be related to poloidal flow velocity [3]. Thus the radial diffusion of test particles D_x is linked to the radial turbulent flux Γ_{n0} and poloidal flow. Eq. 6 is derived under the assumption that correlations between the fluid part of the potential vorticity $\zeta = \nabla^2\phi - n$ and its initial value ζ_0 vanish assymtotically. When correlations do not vanish, the diffusion coefficient can be functions of time, leading to non-diffusive transport. In Fig. 5 we show how the normalised correlation $\langle \zeta_0 \zeta \rangle / \sqrt{\langle \zeta_0^2 \rangle \langle \zeta^2 \rangle}$ evolves with time in the saturated turbulent state for $C = [-0.5, -0.3, 0]$. In all cases, there is an initial phase where correlations decay, corresponding to the initial ballistic

phase of the test particle transport. After this phase, for the $C = -0.3$ and $C = 0$ cases, the correlation fluctuates around zero and the test particle transport is diffusive. For the $C = -0.5$ case, however, correlations persist for long times and the test particle transport is non-diffusive.

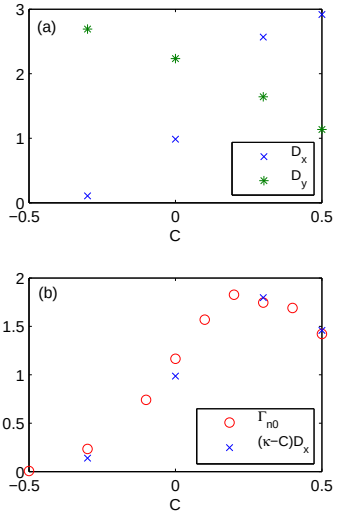

Figure 4: (a) Time independent D_x and D_y.
(b) Average radial density flux Γ_{n0} and $(\kappa - C)D_x$.

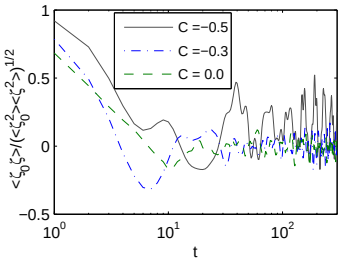

Figure 5: Correlation between ζ_0 and ζ at time t.

Summary. We have studied an extended form of the Hasegawa-Wakatani model that includes the effects of a magnetic field inhomogeneity in the radial direction $B(x)$. The parameter C, controlling the radial gradient of the magnetic field $B(x)$, alters the properties of the turbulence and the dispersion of test particles. The change in turbulent transport is clearly seen in the distribution and skewness of turbulent $E \times B$ density flux Γ_n. Since density n and potential ϕ fluctuations are close to Gaussian, the increase in skewness can be attributed to the increase in phase shifts between n and ϕ, reflecting the transition from drift wave turbulence to drift-interchange type turbulence. Measurements of diffusion coefficients show that the rate of radial transport of test particles increases and the rate of poloidal transport decreases monotonically with C. For large negative values of C, correlations in the flow persist for long times and the radial transport becomes subdiffusive while the poloidal transport becomes superdiffusive. The rate of radial diffusive test particle transport and the average $E \times B$ density flux can be linked by a simple expression, in the form of Fick's law.

Acknowledgements. This work was supported in part by the EPSRC and by Euratom. JMD acknowledges support from an EPSRC CASE studentship in association with UKAEA. The content of the publication is the sole responsibility of the authors and it does not necessarily represent the views of the Commission of the European Union or their services.

References

[1] B.A. Carreras, C. Hidalgo, E. Sanchez, M.A. Pedrosa, R Balbin, I. Garcia-Cortes, B.Ph. van Milligen, D.E. Newman and V.E. Lynch, Phys. Plasmas **3**, 2664 (1996).

[2] R. Basu, T. Jessen, V. Naulin and J. Juul Rasmussen, Phys. Plasmas **10**, 2696 (2003).

[3] J.M. Dewhurst, B. Hnat and R.O. Dendy, Phys. Plasmas, in press (2009).